RESEARCH   **Open Access**

Chronic lung disease in paediatric patients: Does magnetic resonance imaging has a role?

Rania S. M. Ibrahim* and Mona A. F. Hafez

Abstract

Background: Pediatric chronic lung disease (CLD) refers to a range of distinct clinical and pathological disorders that affect children. High-resolution CT (HRCT) is critical for detecting and characterizing parenchymal abnormalities as well as determining their nature and distribution. Although magnetic resonance imaging (MRI) shows promising results, however, due to its poor spatial resolution and signal-to-noise ratio, imaging of the lung parenchyma remains a challenge. As a result, in addition to the initial CT, a follow-up MRI is required. The goal of this paper is to highlight the main imaging features of children with CLD and to evaluate the efficacy of MRI lungs in the diagnosis and monitoring of pediatric CLD.

Results: There was a strong positive correlation between CT and MRI, with a significant P-value. Findings of HRCT and MRI showed a qualitative agreement of 78% complete agreement. MRI helped primary diagnosis in 54% of cases compared to CT in 91% of cases.

Conclusion: MRI lungs are an equivalent technique to HRCT in assessing pediatric CLD; using the modified Helbich–Bhalla score, a strong correlation is obvious between both in the overall assessment. MRI is beneficial for case surveillance rather than primary diagnosis.

Keywords: Chronic lung disease, Magnetic resonance imaging, Computed tomography, Pediatric

Background

Pediatric CLD is an abroad term that encompasses a heterogeneous group of different clinicopathological disorders that advance slowly over months or years [1]. They can broadly be divided into two groups: those with a known cause and those without. Cystic fibrosis, broncho-pulmonary dysplasia or lung of prematurity, asthma, chronic gastroesophageal reflux/aspiration pneumonitis, and constrictive obliterative bronchiolitis, chronic infection, and hypersensitivity pneumonitis are all included in the first group. The second group is subdivided into primary pulmonary diseases (idiopathic interstitial pneumonia, persistent tachypnea of infancy associated with neuroendocrine cell hyperplasia, pulmonary lymphatic

and vascular disorders, etc.) and systemic diseases with a pulmonary manifestation (e.g., Langerhans cell histiocytosis, vasculitides, and granulomatosis) [2]. After the chest radiograph, HRCT is the cornerstone of further imaging studies. It is crucial for detecting and characterizing parenchymal abnormalities, as well as their nature and distribution. It determines the diagnosis, the extent of the disease, and even the therapeutic outcomes [3]. The use of MRI to examine the thoracic vascular structures has shown good results and is gaining popularity. However, because to the poor spatial resolution and SNR of air-filled structures, imaging of the lung parenchyma remains difficult. The use of MRI as the single imaging modality for initial diagnosis is relatively uncommon [1]. Several studies use technique optimization and dose minimization for pediatric chest cases, which are still critical in children [4]. The use of MRI as the sole imaging modality for primary diagnosis is still not widely practiced [1]. Several studies implement technique

*Correspondence: raniasaberm@hotmail.com
Radiology Department, Faculty of Medicine, Pediatric Unit, Kasr El-Ainy Hospital, Cairo University School of Medicine, Kasr Al-aini Street, Al-Manial District, Cairo 11562, Egypt

optimization and dose minimization for pediatric chest cases that remain of paramount importance in children [4]. This article highlights the key imaging manifestations of common pediatric CLD and evaluates them and assesses the efficacy of MRI lungs in the diagnosis or surveillance of pediatric CLD in comparison with HRCT chest (Fig. 1).

Patients and methods

Patients

This is a cross-sectional study that included 70 pediatric patients, 58 males (83%) and 12 females (17%), the age ranged from 1.2 to 14 years old, and the patients referred from the pediatric chest department with chronic chest complain for diagnosis or follow-up during 2 years between January 2018 and March 2020. The cases enrolled in this study are based on the pediatric age group having a history of chronic respiratory symptoms and HRCT evidence of CLD; however, we excluded any cases with acute chest conditions. Also, patients that had severe dyspnea would entangle MRI image quality. The study protocol was approved by the Research Ethical Committee, University Children Hospital. All patients or patients' guardians were counseled and signed a consent form. All cases were subjected to full clinical data including age, sex, clinical complaint, and relevant laboratory investigation was done (Fig. 2).

Method

HRCT chest was done to all patients in the pediatric radiology department, using multi-slice CT 16 Channels helical (GE Bright speed Elite). Patients were in supine, fixed inspiration, and the arms are extended over-head. The scanned area from the top of lungs to the bottom of lungs by instructing the patient to hold the breath at inspiration in cooperative patients however, for uncooperative children, quiet respiration during light universally approved sedative as chloral hydrate was administered. Using the following parameters: 100 kV, 199 mA, helical scan, 1.25 slice thickness, and 5 mm interval. CT chest assessed at lung window 1500 WW, -500 WL, and mediastinal window 400 WW, 60 WL, 2D coronal and sagittal planes, and minimum intensity projection for better assessment of disease extent (Fig. 3).

MRI lungs were done within a period of 1 to 3 days maximum difference, using a 1.5-Tesla superconducting scanner (Magnetom Aera, Siemens Healthineers, Germany). A 6-channel body array coil supporting a parallel imaging technique was used. Applying respiratory gating in young children and end -inspiratory breath-holding in older children; the following parameters are used: T2-weighted sequence FSE (True FISP) axial and coronal, T2-weighted sequence HASTE axial and coronal, T2-weighted sequence blade axial, diffusion-weighted axial cuts, T1-weighted sequence VIBE with and without
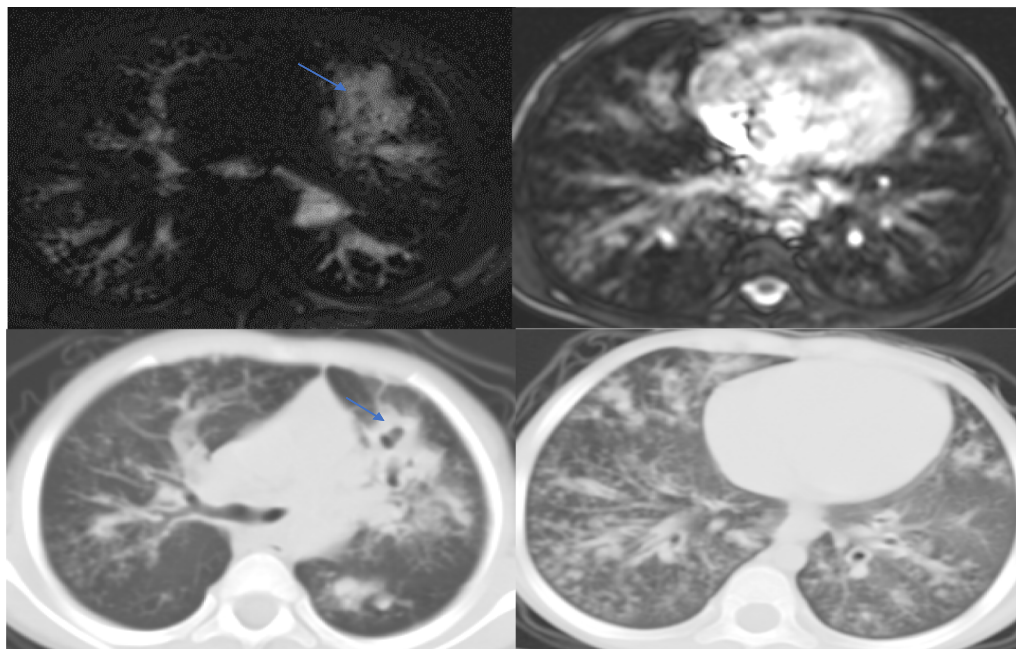

Fig. 1 A 5-year-old male, known with cystic fibrosis, MRI T2 TRUFI, and comparable HRCT cuts, shows bilateral score 1 bronchiectasis, score 2 bronchial wall thickening, score 3 generation of bronchi, diffuse centrilobular nodules and tree in bud appearance, and mucoid impaction (arrows), CT score 21, MRI score 17
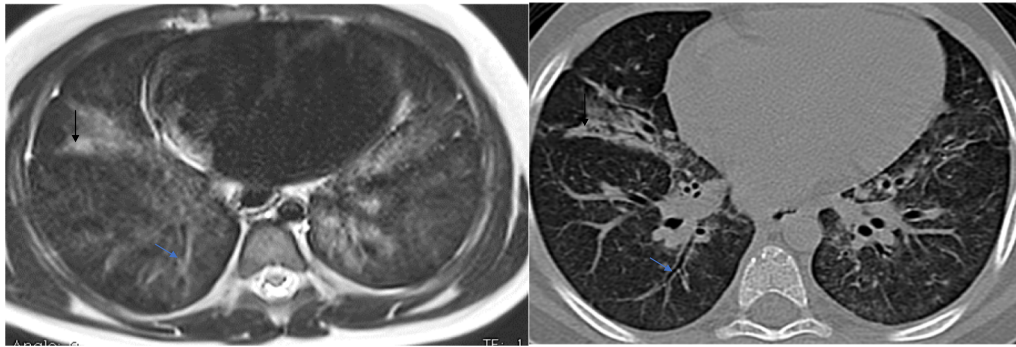
Fig. 2 Male child with history of chronic aspiration due to esophageal dysmotility, T2 HASTE, and comparable HRCT cut; both show the score 1 bronchiectasis and bronchial wall thickening, score 2 bronchial generation (blue arrows), mucoid impaction (black arrows), ground-glass densities and centrilobular nodules, more delineated in HRCT (arrowhead). CT score 14, MRI score 10
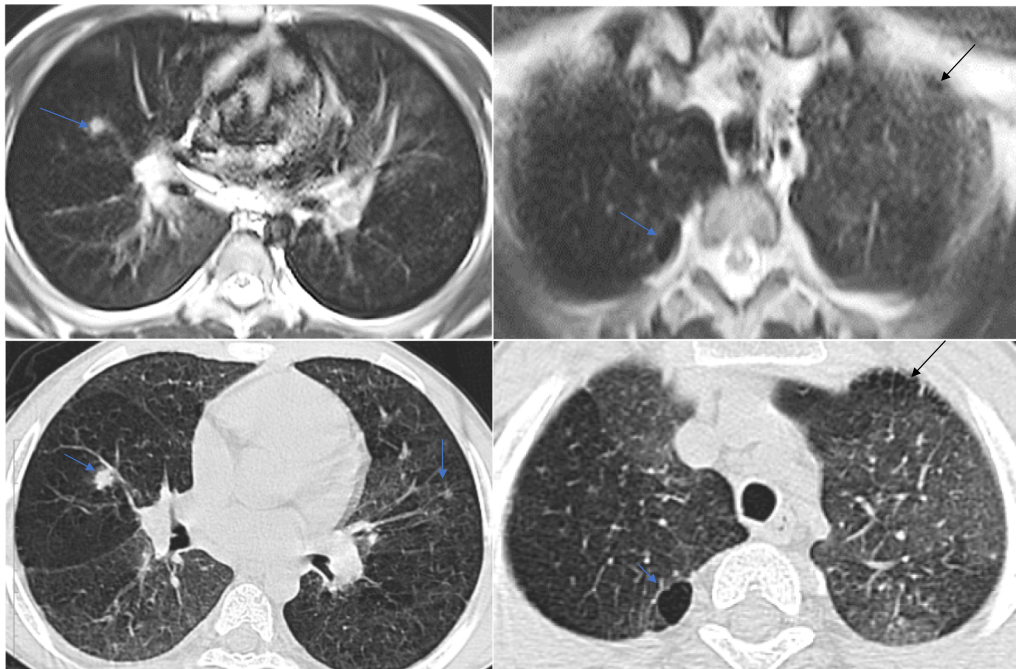

Fig. 3 A 11-year-old male with chronic airway disease secondary to autoimmune disease, T2 HASTE, and comparable HRCT cut; both show the middle lobe air trapping, bilateral nodules better delineated by CT (blue arrows), and bilateral apical subpleural blebs (black arrows). CT score 12, MRI score 9

fat suppression, and T1-weighted sequence in and out-of-phase sequences (Fig. 4).

CT and MRI images analysis were evaluated separately and blindly by two pediatric and chest radiologists with 15 years of experience. With HRCT being the gold standard examination, comparative evaluation of the two studies was done using the modified Bhalla scoring system to facilitate the interpretation of the imaging findings described by Judge et al. [5]; then, by the aid of

clinical data primary diagnosis is tried to be postulated for HRCT and MRI study separately and the final diagnosis concluded after laboratory investigation in cases with granulomatous and cystic fibrosis (CF) disease, and biopsy for cases with interstitial lung disease (ILD).

Statistical analysis

Data were coded and entered using the statistical package SPSS (Statistical Package for the Social Sciences) version
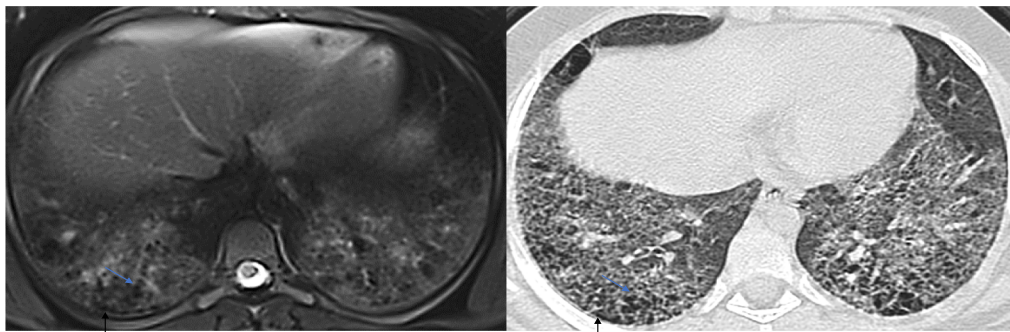
Fig. 4 A 10-year-old female diagnosed as interstitial pulmonary fibrosis (usual interstitial pneumonia), T2 blade, and comparable HRCT cut; both show bilateral fairly symmetrical basal reticulations, interlobular septal thickening, traction bronchiolectasis (blue arrows), bronchial wall thickening, and honeycombing (black arrows). CT score 18, MRI score 20

25. Data were summarized using mean, standard deviation (SD), minimum and maximum in quantitative data, and using frequency (count) and relative frequency (percentage) for categorical data. Correlation of CT and MRI scores using Pearson Correlation Coefficient Calculator then calculated P value; $P < 0.05$ was considered statistically significant. We calculated the mean difference between CT and MRI scores and their SD.

Results

Seventy children with CLD were assessed from January 2018 to March 2020, and the patients consisted of 58 males (83%) and 12 females (17%), with a male-to-female ratio (4.8:1), age ranging 1.2 to 14 years old (mean 5.7). All cases diagnosed as CLD which was 17% subacute hypersensitivity pneumonitis, 26% chronic interstitial lung disease (ILD) {non-specific interstitial pneumonia; (NSIP), and usual interstitial pneumonia; (UIP)}, CF in 8.6%, follicular bronchiolitis in 8.6%, aspiration pneumonia in 25.7%, bronchiolitis obliterans in 5.7%, and chronic granulomatous infection was found in 11.4%. All cases had variable degrees of bronchiectasis, and bronchial wall thickening, 88.6% of cases had ground-glass densities, 57% of cases had mucus plugs and mosaic attenuation, and 51.4% had acinar (centrilobular) nodules. Less frequently, we found fibrosis, honeycombing, air trapping, collapse, consolidation, abscess, sacculation, emphysema, and air bubbles.

The mean modified Helbich–Bhalla score for HRCT was 11.2 (range 3–21, SD 5.3) and that for MRI was 10.46 (range 4–20, SD 4.4), with the mean difference of 0.74 points (a maximum of 48 points could be achieved). There was a strong positive correlation between CT and MRI, with ($R = 0.8366$, and significant P-value < 0.00001). Besides this, there was a strong correlation for bronchiectasis, mucus plugging, peri-bronchial thickening, acinar nodules, ground-glass densities, and mosaic attenuation. The individual agreement of the score values was analyzed, and the results are summarized in Table 1. Findings of HRCT and MRI showed a qualitative agreement of 78% complete agreement, a difference of 1 point appeared in 18.3%, and a deviation of more than 1 point was shown in only 3.7% of patients, with an underestimation by MRI in 11.8% and an overestimation by MRI in 10.2% of the subjects. In the analysis of agreement between the tests, Cohen's kappa was 0.689 and the overall agreement was 85%. MRI overestimated the detection of bronchiectasis, severity, peri-bronchial thickening, extent, presence of mucus plugs, and generalities of disease involvement.

However, HRCT exceeded MRI in the detection of ground-glass opacifications, presence of air bubbles, air trapping, emphysema, mosaic perfusion, presence of fibrosis, interlobular septal thickening, collapse or consolidation, and acinar nodules. Both HRCT and MRI had a 100% agreement in the detection of abscesses or sacculation, and the presence of honeycombing. MRI helped in primary diagnosis in 54% of cases compared to CT in 91% of cases.

With the assist of clinical data, HRCT aided in the primary diagnosis of 91% of cases, as CF and granulomatous disease cases required further laboratory assessment; however, MRI aided in the primary diagnosis of 54% of cases as the distribution and characterization of ground-glass opacification limited the diagnosis of cases with subacute hypersensitivity pneumonitis and NSIP.

Discussion

Pediatric CLD encompasses a diverse range of clinicopathological conditions. It has a long-term, slow-progressing course. More than half of all instances of pediatric CLD occur in children under the age of five [1].

Table 1 The individual agreement and deviation points of scores

	Total number of positive cases	Cases with same point of score	Deviation of point score			
			− 2	− 1	+ 1	+ 2
Severity of Bronchiectasis	70	56	0	3	4	0
Peri-bronchial thickening	70	46	0	0	12	0
Extent of bronchiectasis	70	56	0	0	7	0
Generalities of the bronchial division involved	70	40	0	2	13	0
Extent of mucus plugs	40	40	0	2	9	4
Abscesses or sacculation	6	70	0	0	0	0
No. of bubbles	16	64	3	0	0	0
Emphysema	6	64	0	3	0	0
Collapse/consolidation	14	62	0	2	2	0
Mosaic perfusion/attenuation	40	38	3	13	0	0
Fibrosis, intralobular septal thickening	24	54	0	8	0	0
Honeycombing	4	70	0	0	0	0
Air trapping	20	50	3	7	0	0
Acinar nodule	36	56	0	7	0	0
Ground-glass density	62	52	7	0	2	0
Mean		27.3 (78%)	1 (2.9%)	3.1 (8.9%)	3.3 (9.4%)	0.3 (0.8%)

HRCT is the preferred imaging modality because of its speed, availability, and familiarity, as well as its ease of use, excellent natural contrast, and spatial resolution of the lung parenchyma. MRI has had limited clinical use due to low signal intensity from the lung parenchyma, as well as the prolonged acquisition time and susceptibility to respiratory motion. The lack of radiation makes pulmonary MRI an excellent primary imaging modality for pediatric evaluations, particularly for patients who require serial and longitudinal follow-up, such as CLD patients. Thankfully, new MRI techniques, such as ultra-short echo time and zero echo time, are increasing the number of clinical applications for pulmonary MRI. These sequences provide a greater SNR from the lung's relatively short $T2^*$ due to the use of multi-coil parallel acquisitions and acceleration methods, making pulmonary MRI useful for evaluating lung parenchymal disorders [6].

Different MRI sequence protocols have been raised in the literature. Puderbach et al. provide a comprehensive description of the sequence protocols employed [7]. T2-weighted sequences are the foundation of lung MRI; they are sufficient for morphological diagnosis and are robust. According to recent publications, the most frequently described HASTE sequences are triggered T2-weighted TSE sequences with extended echo-train T2-weighted HASTE sequences. The thickness of the slices should not exceed 5 mm. Pulse triggering is required. Additional respiratory triggering can be done; however, this will increase the time to approximately 30 min [8]. Ventilation and perfusion maps can be generated using Fourier decomposition MRI. Ventilation maps are also produced via multi-volume acquisitions followed by measurement of signal intensities linked to inhalation. This is especially beneficial for children who suffer from severe asthma [9]. Use T1-weighted two- or three-dimensional GRE sequences instead, especially when investigating older children. Due to the short duration of the individual sequence, breath-hold acquisitions become possible. Signal loss due to susceptibility variations can be significantly decreased by using appropriate parameters (low echo time of TE < 1.0 ms) [8].

CT scoring systems exist to grade findings and monitor disease progression. A unique score for MRI does not yet exist and is still being developed. So far, the descriptive report and comparative analysis of images has been the only way of assessing the course of disease [10].

Since 1991, Bhalla scoring system has been used for HRCT scoring of CF lung disease [11], with updates to include other HRCT abnormalities [12, 13]. In the current study, the fourteen parameters of the modified Bhalla scoring system described by Judge et al. were evaluated [5]. The mean modified Helbich–Bhalla score for HRCT was 11.2 (range 3–21, SD 5.3) and that for MRI was 10.46 (range 4–20, SD 4.4), with the mean difference of 0.74 points.

In CLD as CF, many authors found a strong association between CT and MRI [10, 14, 15]. In CF, Teufel

et al. found a strong correlation between CT and very-short echo time MRI (R = 0.87, p 0.01). The average Helbich–Bhalla score for CT was 12.2 [16].

In the current study, there was a strong positive correlation between CT and MRI, with (R = 0.8366, and significant P-value 0.00001) and an overall substantial agreement between the tests, Cohen's kappa was 0.689, and the overall agreement was 85%. These results were compared with a study done by Teufel et al. [16], who used the Helbich–Bhalla score, and they found a strong connection (R = 0.87). Müllera et al. reported a perfect agreement in ILD, with Cohen's kappa of 0.704 and a 91% overall agreement [17].

Although there was a strong correlation between the presence of abscesses or sacculation and the presence of honeycombing in this study, MRI overestimated detection of bronchiectasis, severity, peri-bronchial thickening, extent, presence of mucus plugs, and bronchial generation involvement by 3.6 mean point score in a few cases, this result was in agreement with a study done by Puderbach et al. [18].

Onho and coworkers found nearly perfect agreement in imaging honeycombing, traction bronchiectasis lung nodular, mass lesions, ground-glass, and consolidation opacities, as well as good agreement in visualizing emphysema, air bullae, and reticular opacities [19]. Teufel et al. discovered a strong correlation between peri-bronchial thickening and peripheral mucus plugging, as well as between bronchiectasis, mucus plugging, peri-bronchial thickening, and consolidation in their study [16].

By a mean point score of 4.1, HRCT exceeded MRI in detecting ground-glass opacifications, air bubbles, air trapping, emphysema, mosaic perfusion, presence of fibrosis, interlobular septal thickening, collapse or consolidation, and acinar nodules. This could be explained by the fact that the MRI SNR of normal lung parenchyma is insufficient for distinguishing normal tissue areas from areas with trapped air. A more straightforward approach could be to add a sequence with a very short TE to provide sufficient signal intensity from normal and pathological lung tissue in multiple breath-holds [16].

To reach the ultimate diagnosis, clinical data, along with HRCT and further laboratory tests as well as biopsy, were required. Although, in this study, MRI characterized the granulomatous disease lesions, however, it did not provide a definitive diagnosis, According to Kapur et al., MRI assisted in the detection of tuberculous lesions and suggested that it may be a good alternative instead of performing repeated CT scan for further evaluation of affected children [20].

Limitation of the study is regarding the selection of cases because CT scans were taken with advanced clinical indications in the majority of cases, so there might

have been extensive severity and extent of the appearance of pulmonary changes in these patients and this might provide the better agreement of the results. However, considering a strong correlation between cross-sectional imaging and final diagnosis, we can generally assume that we have a reliable predictive value.

Conclusion

In the gross assessment of pediatric patients with CLD, MRI lungs are comparable to HRCT; however, HRCT is superior in giving fine details of the lung parenchyma and airways. In most morphological alterations and overall assessment using the modified Helbich–Bhalla score, there was a strong correlation between MRI and CT, with a high agreement. Instead of primary diagnosis, it could be useful for case surveillance. Regarding regular follow-up imaging and a rising life span of CLD patients, the positive absence of radiation exposure should not be neglected.

References
1. Rossi UG, Owens CM (2005) The radiology of chronic lung disease in children. Arch Dis Child 25:601–607

2. Deutsch SH, Young LR, Deterding RR, Fan LL, Dell SHD, Bean JA et al (2007) Diffuse lung disease in young children: application of a novel classification. Am J Respir Crit Care Med 176:1120–1128
3. Owens C (2004) Radiology of diffuse interstitial pulmonary disease in children. Eur Radiol 14:2–12
4. Serai SD, Rapp JP, States LJ, Lee EY, Andronikou S, Ciet P et al (2021) Pediatric lung MRI: currently available and emerging techniques. Am J Roentgenol 2021(216):781–790
5. Judge E, Dodd J, Masterson J, Gallagher CHG (2006) Pulmonary abnormalities on high-resolution CT demonstrate more rapid decline than FEV1 in adults with cystic fibrosis. Chest 130:1424–1432
6. Hatabu H, Ohno Y, Gefter WB, Parraga G, Madore B, Lee KS et al (2020) Expanding applications of pulmonary MRI in the clinical evaluation of lung disorders: fleischner society position paper. Radiology 297:286–301
7. Puderbach M, Hintze C, Ley S, Kauczor HU, Biedere J (2007) MR imaging of the chest: a practical approach at 1.5 T. Eur J Radiol 64:345–355
8. Hirscha W, Sorgea I, Krohmer S, Weber D, Meier K, Till H (2008) MRI of the lungs in children. Eur J Radiol 68:278–288
9. Capaldi DPI, Sheikh K, Eddy RL, Guo F, Svenningsen S, Nair P et al (2017) Free-breathing functional pulmonary MRI: response to bronchodilator and bronchoprovocation in severe asthma. Acad Radiol 24:1268–1276
10. Altes TA, Eichinger M, Puderbach M (2007) Magnetic resonance imaging of the lung in cystic fibrosis. Proc Am Thorac Soc 4:321–327
11. Bhalla M, Turcios N, Aponte V, Jenkins M, Leitman BS, McCauley DI et al (1991) Cystic fibrosis: scoring system with thin-section CT. Proton MRI appearance of cystic fibrosis: comparison to CT. Radiology 179:783–788
12. Helbich TH, Heinz-Peer G, Eichler I, Götz M, Wojnarowski C, Brasch RC et al (1999) Cystic fibrosis: CT assessment of lung involvement in children and adults. Radiology 213:537–544
13. De Jong PA, Ottink MD, Robben SG, Lequin MH, Hop WCJ, Hendriks JJE et al (2004) Pulmonary disease assessment in cystic fibrosis: comparison of CT scoring systems and value of bronchial and arterial dimension measurements. Radiology 231:434–439
14. Sileo C, Corvol H, Boelle P, Blondiaux L, Clement A, Le Pointe HD (2014) HRCT and MRI of the lung in children with cystic fibrosis: comparison of different scoring systems. J Cyst Fibros 13:198–204
15. Puderbach M, Eichinger M, Gahr J, Ley S, Tuengerthal S, Schmähl A et al (2007) Proton MRI appearance of cystic fibrosis: comparison to CT. Eur Radiol 17:716–724
16. Teufel M, Ketelsen D, Fleischer S, Martirosian P, Graeber U, Stern M et al (2013) Comparison between high-resolution CT and MRI using a very short echo time in patients with cystic fibrosis with extra focus on mosaic attenuation. Respiration 86:302–311
17. Müller CS, Warszawiak D, Paiva ES, Escuissato DL (2017) Pulmonary magnetic resonance imaging is similar to chest tomography in detecting inflammation in patients with systemic sclerosis. Rev Bras Reumatol 57:419–442
18. Puderbach MU, Wielpütz MO, Von Stackelberg O, Stahl M, Jobst BJ, Eichinger M et al (2018) Multicentre standardization of chest MRI as a radiation-free outcome measure of lung disease in young children with cystic fibrosis. J Cystic Fibrosis 17:518–527
19. Ohno Y, Koyama H, Yoshikawa T, Seki SH, Takenaka D, Yui M et al (2016) Pulmonary high-resolution ultrashort TE MR imaging: Comparison with thin-section standard- and low-dose computed tomography for the assessment of pulmonary parenchyma diseases. J Magn Reson Imaging 43:512–532
20. Kapur S, Bhalla AS, Jana M (2019) Pediatric chest MRI: a review. Indian J Pediatr 86(9):842–853

Publisher's Note